Sainmatika: Jurnal Ilmiah Matematika dan Ilmu Pengetahuan Alam
Volume 21 No. 2, December 2024 DOI 10.31851/sainmatika.v21i2.16722
https://jurnal.univpgri-palembang.ac.id/index.php/sainmatika

Optimization of Palm Shell Drying to Enhance Adsorption Performance: A Kinetic Study and Exponential Model

Surya Hatina[1], Dian Sari Dewi[2], Alfina[3], Sisnayati[4], Dewi Putri Yuniarti[5], Ria Komala[6*]
*e-mail: ria.komala0411@gmail.com

[1,2,3,4,5,6*]*Department of Chemical Engineering, Faculty of Engineering, Universitas Tamansiswa Palembang, Indonesia*

ABSTRACT

Palm shell has great potential as an adsorbent material due to its porosity and thermal stability, but its high moisture content can affect its surface area and absorption capacity. This study aims to optimize the drying process of palm shells to enhance their adsorption performance by applying an exponential model. The drying process was carried out at a temperature of 80°C with time variations ranging from 1 to 6 hours. Parameters measured included wet and dry moisture content, Moisture Ratio (MR), and drying rate. The results showed that drying the palm shell for 4 hours yielded the best results, with a reduction in wet moisture content by 19-21% and dry moisture content by 23-28%. The exponential model analysis provided drying rate constants for the three samples of 0.0443, 0.0238, and 0.0159, respectively. The measured MR graph compared with the model predictions showed a very good fit, with an R^2 value close to 1, meaning the exponential model is effective in predicting the drying rate. Adsorption performance was tested using a Dylon dye solution with a concentration of 25 ppm, where the palm shell was able to adsorb up to 85% of the dye within 180 minutes.

Keywords: Palm Shell, Drying, Adsorption, Moisture Ratio, Exponential Model

INTRODUCTION

Palm oil is one of Indonesia's primary commodities, producing a variety of derivative products, including crude palm oil (CPO) (Setiajiati et al., 2024). However, palm oil processing also generates a significant amount of biomass waste, such as empty fruit bunches, fibers, and palm shells (Dolah et al., 2021). Among these waste types, palm shells are often used solely as boiler fuel in the palm oil industry, despite their considerable potential as natural adsorbents. Palm shells possess high porosity, thermal stability, and significant carbon composition, making them an ideal candidate for adsorption applications in wastewater treatment or air purification (Uchegbulam et al., 2022).

One of the main challenges in utilizing palm shells as adsorbents is that adsorption performance heavily depends on the quality of material preparation. Drying is a crucial step in preparing palm shells because high moisture content can affect the pore structure, surface area, and absorption capacity of the adsorbent (Yek et al., 2019). In the drying process, temperature control, time, and environmental conditions are critical factors that must be optimized to produce effective adsorbent materials (Gayathiri et al., 2022). A lack of understanding of drying kinetics and the appropriate mathematical models often results in trial-and-error drying processes, reducing the efficiency and effectiveness of palm shells as adsorbents.

Many studies have been conducted on biomass drying, both for various types of lignocellulosic materials and other biomass. For example, research by Zhang et al, showed that drying at higher temperatures accelerates water evaporation but can damage the material's pore structure, ultimately reducing adsorption capacity(Zhang et

al., 2022). Another study by Wu et al. (2024) also discussed the use of an exponential model to predict drying rates in biomass materials, but the focus was limited to other types of biomass, such as straw or wood (Wu et al., 2024). To date, studies on palm shell drying using an exponential model and its impact on adsorption performance are still limited.

Although there is extensive research on biomass drying, a specific understanding of palm shell drying kinetics and optimizing the process to enhance adsorption capacity is still lacking. Most previous studies focused more on the physical and chemical characterization of palm shells without directly linking them to drying kinetics and their impact on adsorption performance. Furthermore, the exponential models used in various studies often do not account for the specific conditions of lignocellulosic materials like palm shells.

The novelty of this research lies in combining the study of palm shell drying kinetics with the application of an exponential model to predict the Moisture Ratio (MR) and drying rate. By taking this approach, this study aims to provide precise guidelines for optimizing the drying process to produce high-performance adsorbents. This research not only seeks to enhance the value of palm shells on an industrial scale but also aims to contribute to the biomass drying literature, particularly concerning lignocellulosic materials like palm shells.

The objective of this study is to optimize the drying process of palm shells by studying drying kinetics and applying an exponential model to enhance adsorption performance. Through this study, it is expected to obtain optimal parameters that can be applied on an industrial scale to increase the added value of palm shells as adsorbents.

MATERIALS AND METHODS

Research Materials

The primary material used in this study is palm shells obtained from a palm oil mill at the port dock in Tanjung Api-Api, Banyuasin Regency, South Sumatra. The tools used in this study include a drying oven, an analytical balance, and other supporting equipment.

Material Preparation

The collected palm shells had an average diameter of 5 mm (equivalent to 4 mesh). They were first washed with distilled water (aquadest) to remove any attached foreign particles, then air-dried at room temperature to reduce initial moisture content. Afterward, the samples were dried in an oven at a temperature of 80°C with varying drying times of 1, 2, and up to 6 hours to study the drying kinetics of the palm shells.

Moisture Content Measurement

After drying, the palm shell samples were weighed at each specified time using an analytical balance to determine the weight loss due to water evaporation. Moisture content was measured using the gravimetric method, which compares the wet weight to the dry weight of the palm shells. The Moisture Ratio (MR) was calculated using the following equation (Aksoy et al., 2019)

$$MR = \frac{w_t - w_e}{w_o - w_e} \quad (1)$$

Where:
Wt = Sample weight at time t (g)
We= Equilibrium weight (dry weight) (g)
W_0 = Initial sample weight (g)

Assuming the equilibrium moisture content *We* is zero, the equation simplifies to:

$$MR = \frac{w_t}{w_o} \quad (2)$$

Drying Kinetics Study

The drying kinetics study was conducted by analyzing the changes in Moisture Ratio (MR) over time at each drying temperature. The MR data obtained was used to model the drying kinetics of the palm shells. The modeling applied an exponential model (Alsulami et al., 2023), expressed by the following equation:

$$MR = exp\ (-kt) \quad (3)$$

Where:
k = Drying rate constant (hr^{-1})
t = Drying time (hours)

The drying data at 80°C was then analyzed to determine the drying rate constant (k) at this temperature. A logarithmic plot of the Moisture Ratio (ln MR) versus time was made to assess the suitability of the exponential model in describing the drying behavior of the palm shells.

Adsorption Analysis

After the drying process, the palm shells underwent carbonization, activation, and pillaring, and were tested for their adsorption capability to evaluate the effect of the drying process on adsorption performance. Adsorption was carried out using a test solution, Dylon dye solution (Hb09) at a concentration of 25 ppm, mixed with 1 gram of pillared palm shell activated carbon. The adsorption process was conducted with contact times of 30, 60, 90, 120, 150, and 180 minutes. The color of the solution before and after the adsorption process was measured using the Hach Method No. 8025 in PtCo units.

Data Analysis

The MR data obtained from the measurements were analyzed using linear regression to examine the fit of the exponential model to the experimental data. Additionally, statistical analysis was conducted to determine the significant effects of drying time on the drying rate and adsorption capacity.

RESULTS AND DISCUSSION

1. **Wet Moisture Content and Dry Moisture Content**

Wet Moisture Content and Dry Moisture Content are two important parameters used to measure the amount of water in a material during the drying process (Macedo et al., 2024). These parameters provide different perspectives on how much water remains in the material and how effective the drying process is.

Table 1 shows data on the reduction of moisture content in palm shells during the drying process. By examining the wet and dry moisture content at different time intervals, the optimal point can be determined where drying reaches maximum efficiency—when the moisture content in the sample decreases significantly and stabilizes.

Table 1. Wet and Dry Moisture Content in Palm Shells During the Drying Process

Sample	t (hours)	Wet Weight (Wb)	Weight at Time Interval (Wd)	Wet Moisture Content	Dry Moisture Content
Palm Shells 1	1.00	537.04	493.70	8.07%	8.78%
	2.00	537.04	459.57	14.43%	16.86%
	3.00	537.04	444.38	17.25%	20.85%
	4.00	537.04	435.65	18.88%	23.27%
	5.00	537.04	432.68	19.43%	24.12%
	6.00	537.04	428.52	20.21%	25.32%
Palm Shells 2	1.00	537.05	470.07	12.47%	14.25%
	2.00	537.05	447.75	16.63%	19.94%
	3.00	537.05	437.31	18.57%	22.81%
	4.00	537.05	432.47	19.47%	24.18%
	5.00	537.05	432.29	19.51%	24.23%
	6.00	537.05	430.40	19.86%	24.78%
Palm Shells 3	1.00	523.39	436.03	16.69%	20.04%
	2.00	523.39	419.71	19.81%	24.70%
	3.00	523.39	409.99	21.67%	27.66%
	4.00	523.39	406.25	22.38%	28.83%
	5.00	523.39	405.91	22.45%	28.94%
	6.00	523.39	405.75	22.48%	28.99%

Table 1 shows the measurement results of wet and dry moisture content from three samples of palm shells during the drying process. The drying was conducted at time intervals ranging from 1 to 6 hours. The initial wet weight and the sample weight at each time interval were recorded. From this data, wet and dry moisture content were calculated to understand the drying rate and process efficiency.

Drying is a critical step in preparing palm shell raw materials for the adsorption process. The purpose of drying is to reduce the moisture content in the material, thereby increasing the availability of pores and the active surface area needed for the effectiveness of subsequent processes**.**

Figures 1 and 2 present data on the changes in wet and dry moisture content (% Moisture Content) from three palm shell samples during different drying times, measured hourly until a stable point is reached. This analysis aims to determine the optimal drying time to achieve energy efficiency and maximize results.

p-ISSN 1829 586X
e-ISSN 2581-0170

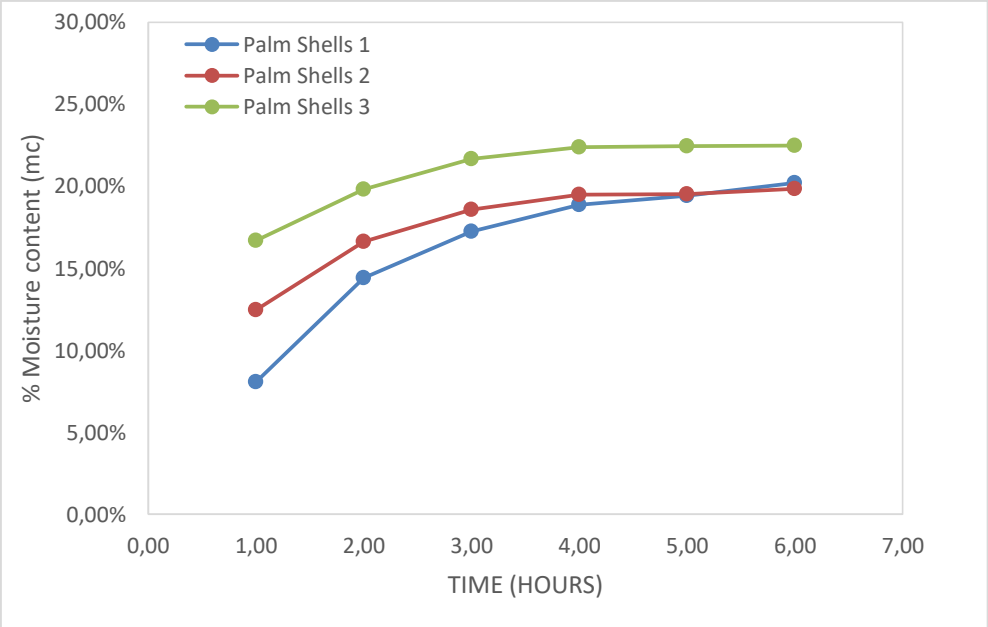

Figure 1. Graph of Wet Moisture Content Percentage

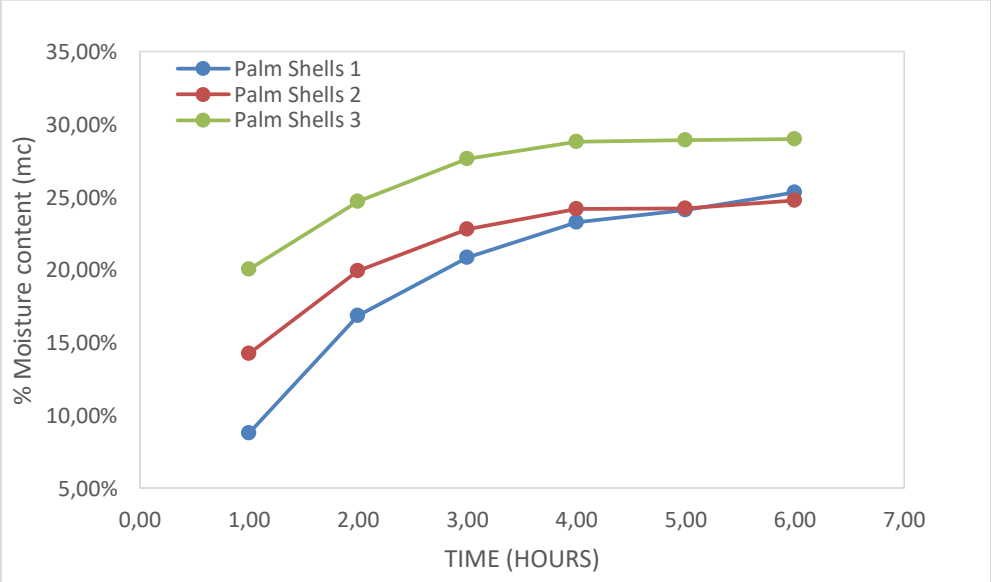

Figure 2. Graph of dry moisture content percentage

Figures 1 and 2 show the changes in wet and dry moisture content of palm shells during the drying process at various times.

Optimal Drying Time for Palm Shells

Figures 1 and 2 illustrate the graphs of changes in wet and dry moisture content in palm shells during the drying process over time. The efficiency of the drying process can be analyzed from the pattern of moisture reduction in both graphs. In Figure 1, the graph displays the wet moisture content (moisture content wet basis). It can be observed that the moisture content of palm shells decreases significantly at the beginning of the drying process. This reduction occurs rapidly during the first 4 hours. After that, the rate of moisture reduction begins to slow down, and the graph shows a leveling trend, indicating that the drying process is reaching its efficiency limit. Figure 2, which shows the dry

p-ISSN 1829 586X
e-ISSN 2581-0170

moisture content (moisture content dry basis), follows a similar pattern. In the early stages of drying, the dry moisture content decreases significantly, especially during the first 4 hours. However, after 4 hours, the moisture reduction slows down, and the graph again shows a leveling trend. This suggests that by this point, most of the water has been evaporated, and additional drying time will only result in a minimal reduction in moisture content. Based on both graphs, it can be concluded that the optimal time to stop drying is 4 hours. At this point, most of the moisture has already been reduced, and extending the drying time will only yield a very small decrease in moisture content with diminishing efficiency.

From an energy efficiency perspective, drying for four hours at the optimal temperature significantly reduces the moisture content without damaging the pore structure of the activated carbon. Excessive drying time or high temperatures can cause pore damage, potentially reducing the material's adsorption capacity. According to the theory of drying porous materials, the optimal drying duration is achieved when the moisture content is sufficiently low to enhance the adsorption capacity, yet without altering the material's pore structure (Yek et al., 2019). Drying for four hours at a controlled temperature results in an optimal moisture content, allowing the activated carbon to maintain its pore structure, which is crucial for the adsorption process.

Wet and Dry Moisture Content Values

The wet and dry moisture content values play an important role in the adsorption process of materials such as palm shells. Figures 1 and 2 provide an overview of the wet and dry moisture content values of palm shells. The adsorption process is influenced by the remaining moisture in the material after drying. The wet and dry moisture content values give an indication of how much water is still bound to the surface and within the pores of the material.

Wet Moisture Content (Moisture Content Wet Basis):

Wet moisture content is calculated based on the percentage of water mass relative to the total wet mass of the material. According to the displayed graph, the wet moisture content of palm shells shows a significant reduction during the first 4 hours of the drying process, decreasing from around 19-21% across various samples. After this point, the reduction in wet moisture content begins to slow, indicating that most of the easily evaporated free water has been removed in the early stages of drying.

Dry Moisture Content (Moisture Content Dry Basis

Dry moisture content is calculated based on the percentage of water mass relative to the dry mass of the material. The graph for dry moisture content also shows a significant reduction in the first 4 hours, around 23-28%. Similar to wet moisture content, after 4 hours, the rate of reduction slows, indicating that the remaining water is more tightly bound within the material's structure.

Based on the moisture content graphs, it can be concluded that the reduction in moisture during the drying process has a direct impact on the performance of palm shells as an adsorbent material. During the early hours of drying, moisture decreases rapidly, opening up the pores and increasing the effective surface area of the palm shells. This will result in greater adsorption capacity as more space becomes available to absorb contaminants. However, once the drying time reaches around 4 to 6 hours, the rate of moisture reduction begins to slow. This suggests that most of the free water

p-ISSN 1829 586X
e-ISSN 2581-0170

has evaporated, and the remaining water is more difficult to remove. Stopping the drying process at this point is optimal to ensure that the palm shells have a sufficiently low moisture content for adsorption without damaging the pore structure. Prolonged drying could risk structural damage that would reduce the material's adsorption capacity. Therefore, lower moisture content, especially after optimal drying, will result in palm shells being more efficient as an adsorbent due to open pores and increased absorption capacity. Proper drying will maximize adsorption potential without wasting energy or compromising the material's integrity (Broda et al., 2021).

The drying process of palm kernel shell as a precursor for activated carbon significantly affects its pore structure and adsorption capacity. Analysis of the wet and dry moisture content during drying shows that the moisture content decreases significantly during the first four hours, with a slower rate of decrease thereafter. This aligns with the drying theory explained by Macedo et al, which states that the initial stage of drying occurs quickly because free water on the surface of the material evaporates more easily, while the final stage requires more time due to the water remaining more capillary-bound within the pores of the material (Macedo et al., 2024)

2. Exponential Drying Model

This study uses a mathematical model to describe the drying process, specifically the exponential model (Thao et al., 2023). In general, this model states that the drying rate follows an exponential function over time, where the rate of water loss is proportional to the remaining moisture content in the material. The Newton model, one of the simplest exponential models, is used in this study to describe the material drying process (Andrade et al., 2022).

Table 2. Table of Moisture Content, Drying Rate, and Moisture Ratio for Palm Shell Drying at 80°C

Sample	T (^oC)	Time(Hours)	Wet Weight (Wb)	Weight at Time Interval (Wd)	Moisture Content /MC (%)	Drying Rate/DR (%)	Moisture Ratio /MR	Ln MR
Palm Shells 1	80	1	537.04	493.7	8.07%	0.00%	1.000	0.000
		2	537.04	459.57	14.43%	6.36%	1.787	0.581
		3	537.04	444.38	17.25%	2.83%	1.196	0.179
		4	537.04	435.65	18.88%	1.63%	1.094	0.090
		5	537.04	432.68	19.43%	0.55%	1.029	0.029
		6	537.04	428.52	20.21%	0.77%	1.040	0.039
Palm Shells 2	80	1	537.05	470.07	12.47%	0.00%	1.000	0.000
		2	537.05	447.75	16.63%	4.16%	1.333	0.288
		3	537.05	437.31	18.57%	1.94%	1.117	0.111
		4	537.05	432.47	19.47%	0.90%	1.049	0.047
		5	537.05	432.29	19.51%	0.03%	1.002	0.002
		6	537.05	430.4	19.86%	0.35%	1.018	0.018
Palm Shells 3	80	1	523.39	436.03	16.69%	0.00%	1.000	0.000
		2	523.39	419.71	19.81%	3.12%	1.187	0.171
		3	523.39	409.99	21.67%	1.86%	1.094	0.090
		4	523.39	406.25	22.38%	0.71%	1.033	0.032
		5	523.39	405.91	22.45%	0.06%	1.003	0.003
		6	523.39	405.75	22.48%	0.03%	1.001	0.001

Table 2 presents experimental data on the drying of palm shells at a temperature of 80°C**.** The data includes the weight of the wet and dry material, moisture content, drying rate, moisture ratio, and the logarithmic value of the moisture ratio

p-ISSN 1829 586X
e-ISSN 2581-0170

(Ln MR) at various drying time intervals. To Model the moisture ratio (MR) using an exponential equation (Eq. 2), the exponential MR values are calculated based on the constant k. This k-value is obtained from the slope of the regression line on the plot of ln MR versus time (Figure 3).

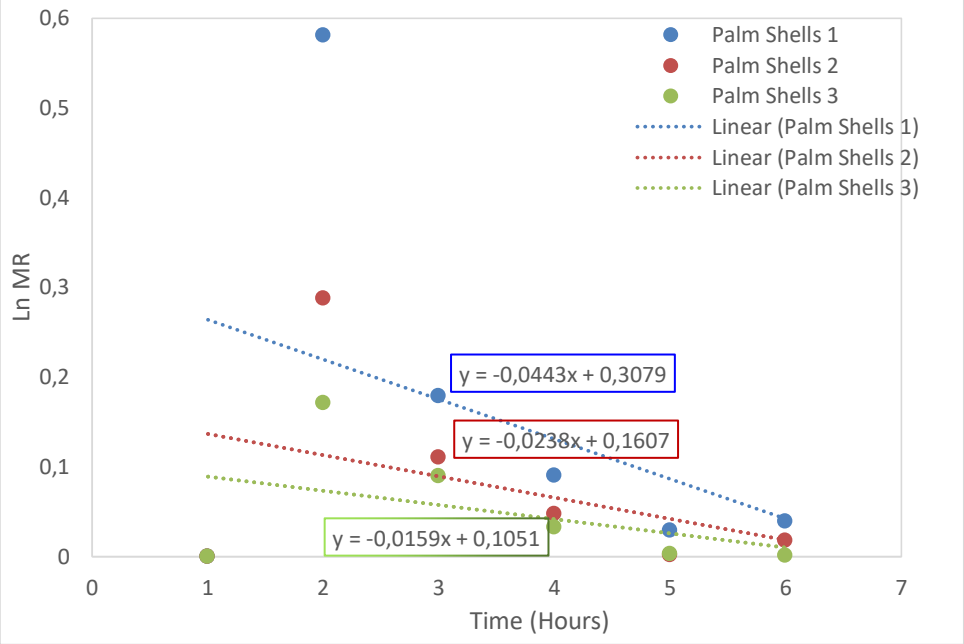

Figure 3. Linear Graph of Ln MR and Time

Figure 3 shows three linear equations illustrating the relationship between drying time (in hours) and the natural logarithm of the Moisture Ratio (Ln MR). These equations are used to determine the drying rate constant (k) and the exponential model of the Moisture Ratio (MR) for each sample. The k-value in the exponential model is obtained from the gradient (slope) of the linear line on the Ln MR versus time graph. The calculation follows Newton's exponential model equation, which is

$$Ln(MR) = -kt + C \quad \ldots\ldots\ldots\ldots (4)$$

A negative value of the drying rate constant k. Thus, the k-values for each sample are as follows:

- **Palm Shell 1**, equation:
- y=−0.0443x+0.3079y, yields k=0.0443
- **Palm Shell 2**, equation:
- y=−0.0238x+0.1607y, yields k=0.0238
- **Palm Shell 3**, equation:
- y=−0.0159x+0.1051y, yields k=0.0159

The k-values are substituted into the exponential equation to obtain the exponential Moisture Ratio (MR) model for each sample. The exponential model for each sample is as follows (Equation 3):

- **Palm Shells 1**: $MR=e^{-0.0443t}$
- **Palm Shells 2**: $MR=e^{-0.0238t}$
- **Palm Shells 3**: $MR=e^{-0.0159t}$

By using the k-values and the corresponding exponential models, the predicted Moisture Ratio (MR) values were obtained from the exponential model (Table 3). This allows us to predict how the moisture content in the samples will decrease over time.

Table 3. Table of Moisture Ratio and Exponential Model Predictions for Palm Shell Drying

Sample	T (°C)	Time(Hours)	Moisture Ratio (MR)	K	Exponential Moisture Ratio (MR) Model
Palm Shell 1	80	1	1.000	0.044	0.957
		2	1.787	0.044	0.915
		3	1.196	0.044	0.876
		4	1.094	0.044	0.838
		5	1.029	0.044	0.801
		6	1.040	0.044	0.767
Palm Shell 2	80	1	1.000	0.024	0.976
		2	1.333	0.024	0.954
		3	1.117	0.024	0.931
		4	1.049	0.024	0.909
		5	1.002	0.024	0.888
		6	1.018	0.024	0.867
Palm Shell 3	80	1	1.000	0.016	0.984
		2	1.187	0.016	0.969
		3	1.094	0.016	0.953
		4	1.033	0.016	0.938
		5	1.003	0.016	0.924
		6	1.001	0.016	0.909

Table 3 presents the measured Moisture Ratio (MR) of palm shells during the drying process at a temperature of 80°C across different drying times. The data also includes the predicted MR values using the exponential model with different drying rate constants k for each experimental sample. The graph generated from this data will show a comparison between the measured MR values and the MR values predicted by the exponential model.

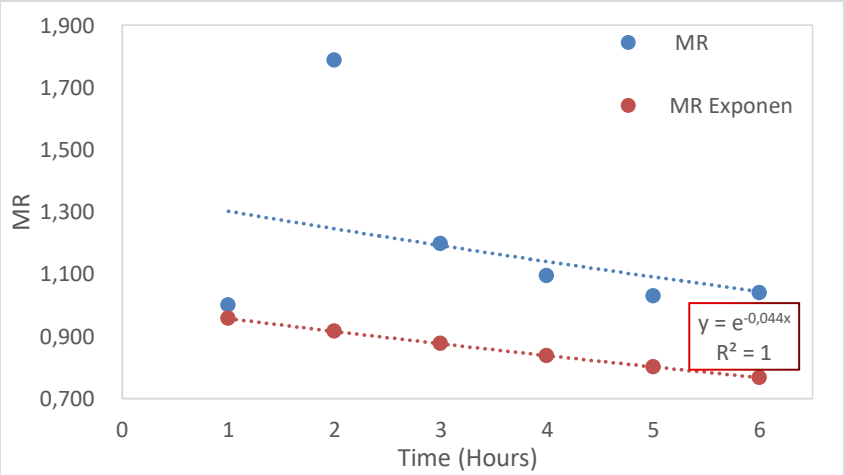

Figure 4. Exponential Drying Model of Palm Shells 1

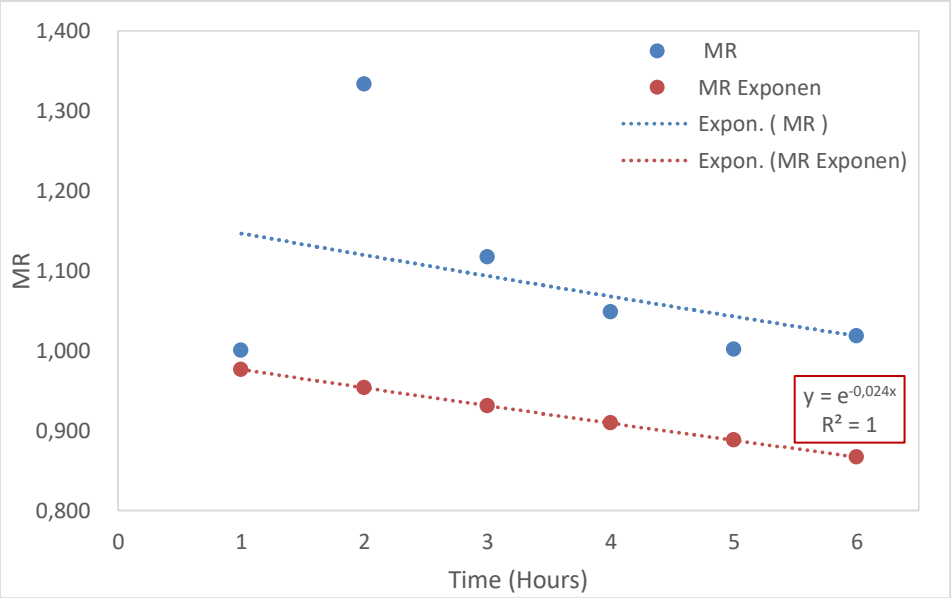

Figure 5. Exponential Drying Model of Palm Shells 2

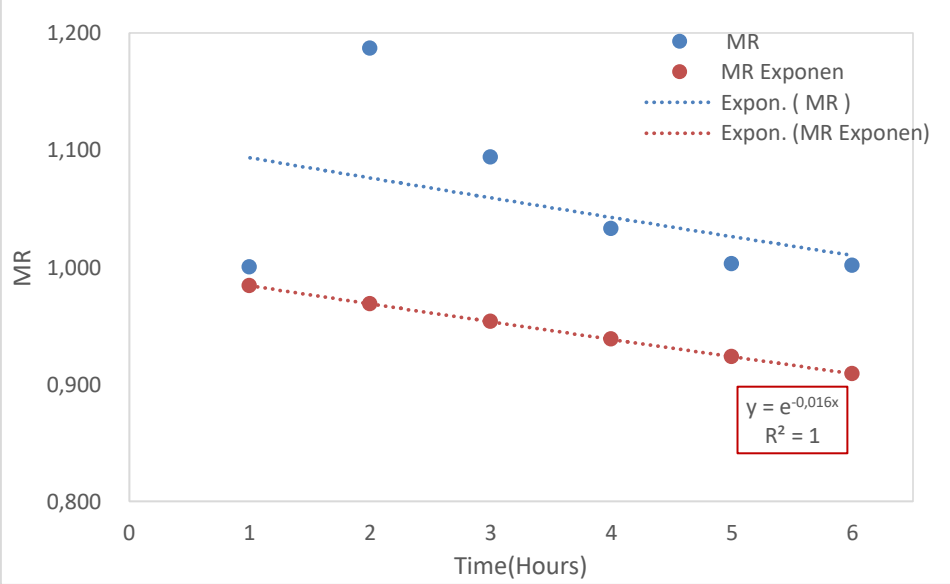

Figure 6. Exponential Drying Model of Palm Shells 3

Figures 4, 5, and 6 show the exponential drying model of palm shells with Moisture Ratio (MR) as the primary parameter measured against drying time (hours). Each graph represents a drying experiment with three different samples (Palm Shell 1, 2, and 3), where the actual MR is represented by blue dots and the modeled exponential MR is represented by orange dots.

Figure 4 illustrates the decline of actual MR and modeled exponential MR during 6 hours of drying for Palm Shell 1. The exponential model is represented by the equation $y=e^{-0.044x}$ with $R^2=1$, indicating a perfect fit between the exponential MR data and the model. The actual MR is slightly higher than the exponential MR at the beginning of drying but decreases consistently after 3 hours, approaching the model's MR.

Figure 5 shows the drying model for Palm Shell 2, with the actual MR decreasing in a similar pattern to Figure 5 but with a higher initial MR. The exponential model is represented by

$y=e^{-0.024x}$ and $R^2=1$, indicating a good model fit. The actual MR tends to be higher than the exponential model at the start, suggesting a slower initial reduction in moisture compared to the model.

Figure 6 presents the drying model for Palm Shell 3, where the MR also follows an exponential pattern with the equation $y=e^{-0.016x}$ and $R^2=1$. Similar to Figures 4 and 5, the actual MR is above the exponential MR at the start but shows a steady decline, approaching the model after 6 hours.

Based on these figures, the graphs demonstrate that the drying process of palm shells generally follows an exponential model, with R^2 values reaching 1 indicating a very good fit between the model and the MR data. However, during the early stages of drying, the actual MR tends to be higher compared to the exponential model. This discrepancy could be due to factors such as non-ideal drying conditions, for example, inconsistent temperature or slow evaporation rates affecting the moisture loss rate.

The slower moisture reduction in the early drying stages might indicate the need for optimization of drying conditions to achieve lower moisture content in a shorter time (Radojčin et al., 2021). The exponential model suggests that after a few hours, the drying rate stabilizes and aligns closely with the model's predictions.

Overall, the results from these graphs suggest that palm shells, after undergoing exponential drying, have good potential as adsorbents. However, optimization in the early drying stages is necessary to enhance the drying rate and maximize adsorption capacity (Boateng & Yang, 2021).

The application of the exponential model in this study shows a high level of agreement between the predicted results and the empirical data, indicating that the exponential model is an effective approach for describing the rate of moisture content reduction during biomass drying. This finding is consistent with the research by Thao et al, which demonstrated that the exponential model can accurately describe the reduction in moisture content in lignocellulosic materials (Thao et al., 2023). In this exponential model, the drying rate constant (k) indicates that moisture content decreases rapidly in the initial stage when free water is still available and slows down in the final stage as bound water begins to evaporate.

3. FTIR Analysis

FTIR (Fourier Transform Infrared Spectroscopy) is a commonly used method for identifying functional groups on material surfaces, including activated carbon. In this context, the activated carbon used is derived from palm shell, which have been metal-pillared specifically to enhance its adsorption capacity for synthetic dye compounds.

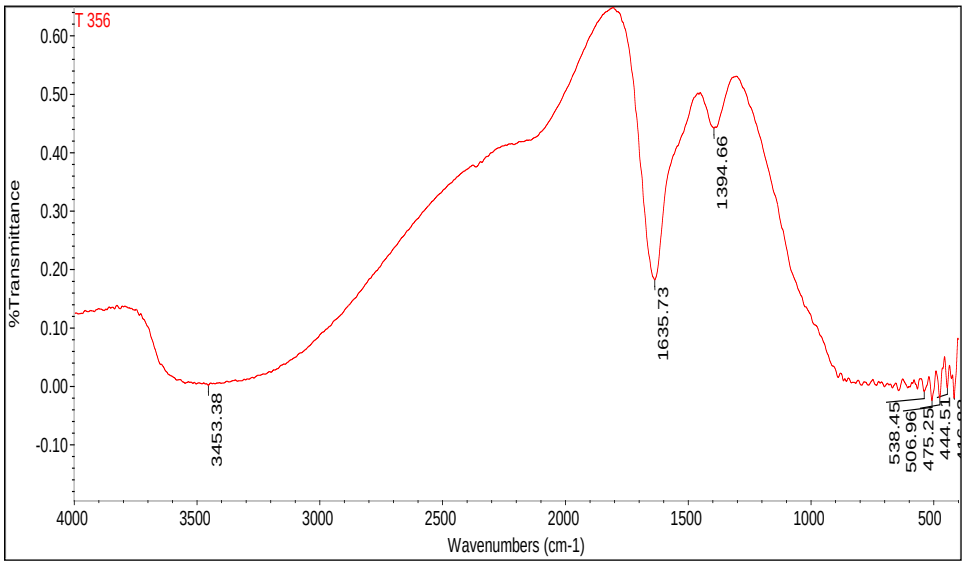

Figure 7. FTIR Spectrum of Metal-Pillared Palm Shell Activated Carbon

The FTIR spectrum of activated carbon from palm shell that has been metal-pillared shows various functional groups on the carbon surface that support its adsorption capacity. In this spectrum, a peak around 3400 cm^{-1} is observed, which is generally associated with the vibration of hydroxyl groups (-OH). This hydroxyl group may come from bound water molecules or hydroxyl groups present on the activated carbon surface, which can aid in interactions with polar compounds. Additionally, the peak around 2900 cm^{-1} indicates the presence of C-H vibrations from alkyl groups, which could be a sign of residual organic compounds from the activated carbon preparation process.

Around 1600 cm^{-1}, a peak appears that may indicate the presence of C=O or C=C bonds, suggesting aromatic or carbonyl structures on the activated carbon surface. Aromatic structures typically indicate the stability of the activated carbon, while carbonyl groups may help enhance the adsorption capacity for specific organic compounds. At lower wavenumber

Regions, around 600-400 cm^{-1}, peaks are observed that can be attributed to metal-oxygen (M-O) vibrations, indicating that the metal-pillaring process on the activated carbon was successfully carried out. The metal incorporated helps to increase the carbon's adsorption ability toward certain compounds, such as synthetic dyes.

Overall, this spectrum shows that the metal-modified activated carbon from palm shell has active groups on its surface that are very useful in the adsorption process. The presence of groups such as -OH, C=O, and M-O indicates that the modification has successfully improved the adsorption capacity of the activated carbon, making it effective for removing specific compounds from solutions.

Recent studies on activated carbon, including those derived from agricultural waste like rice husk, support similar findings regarding the FTIR spectrum of metal-modified activated carbon. For example, research by Mortada et al. highlights the presence of hydroxyl groups (-OH) and aliphatic C-H vibrations in the FTIR spectra, which enhance the adsorption capacity of activated carbon for contaminants such as chemical oxygen demand (COD) in wastewater (Mortada et al., 2023).

p-ISSN 1829 586X
e-ISSN 2581-0170

Similar findings have been reported in other studies, where metal pillaring of activated carbon improved adsorption efficiency by introducing metal-oxygen (M-O) bonds that aid in specific adsorption processes

4. XRD Analysis

Graph 8. shows the X-ray Diffraction (XRD) analysis results of metal-pillared, palm shell-based activated carbon. This graph displays X-ray intensity against the diffraction angle (2θ) with two curves representing the original intensity and the smoothed intensity. This analysis aims to identify changes in the crystal structure of activated carbon after metal pillaring modification, which can affect material properties such as surface area and adsorption capacity.

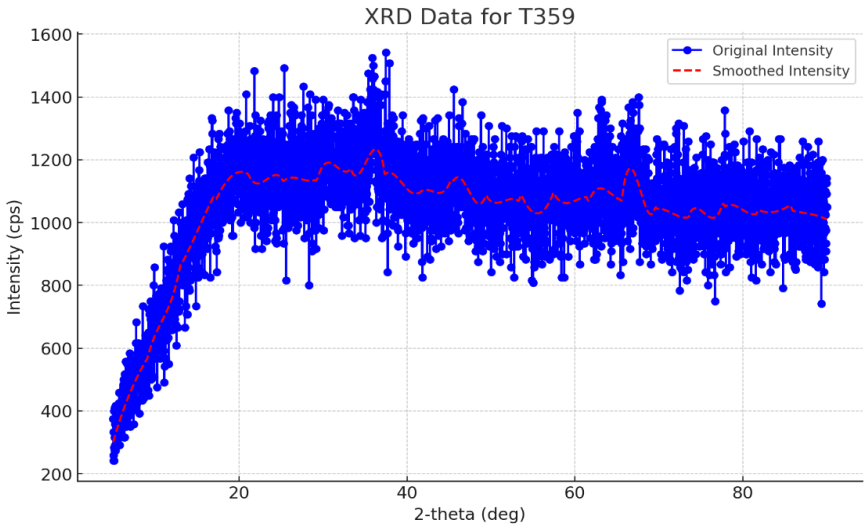

Figure 8. X-ray Diffraction (XRD) analysis results of metal-pillared, palm shell-based activated carbon

The XRD graph of palm shell-based activated carbon that has been metal-pillared shows a characteristic diffraction pattern typical of materials with a mixture of crystalline and amorphous structures. The diffraction pattern displays high-intensity peaks in the 2-theta range between 15° and 40°, indicating the presence of crystalline phases within the modified material. The metal-pillaring process is known to alter the microcrystalline structure of activated carbon, as reported by Bulavchenko et al, where modification with transition metals increased crystallinity at certain angles, thereby enhancing the material's performance in adsorption and catalytic applications. In this graph, there is also a comparison between the original intensity curve and the smoothed curve, showing the base pattern of diffraction intensity without noise, making the main peaks more identifiable (Bulavchenko & Vinokurov, 2023).

The stable intensity distribution at 2-theta angles above 40° suggests a semi-crystalline or even amorphous phase within the activated carbon, as supported by a recent study by Mehdipour et al. They found that metal-pillared activated carbon often has an increased amorphous component, which provides mesoporous characteristics suitable for pollutant adsorption (Mehdipour-Ataei & Aram, 2023). The broad peak in the graph also indicates an amorphous phase, consistent

with findings by Xu et al, where metal-pillared activated carbon showed broad and diffuse diffraction peaks due to the metal distribution within the carbon pores, significantly increasing the surface area of the material (Xu et al., 2018).

Additionally, the crystalline structure achieved through pillaring can enhance thermal stability and catalytic activity, as discussed in research by Yim et al. They found that metal-pillared activated carbon exhibited greater thermal stability and structural resilience, supporting catalytic applications under extreme reaction conditions. With further analysis, such as crystallite size calculations using the Scherrer equation, this study could reveal the distribution of metal particles within the activated carbon structure (Yim & Kim, 2023). This observation aligns with Wang et al, who demonstrated that nanoscale metal distribution increases adsorption and catalytic efficiency due to the greater number of active sites (Wang et al., 2023).

Overall, the XRD results align with recent studies showing that metal pillaring of activated carbon improves crystallinity and mesoporous structure, enhancing the material's potential in environmental and industrial applications, particularly for adsorption and catalysis.

5. Adsorption Process Analysis

The efficiency of the adsorbent in absorbing contaminants from the solution was evaluated through an experiment using a synthetic dye solution, where 1 gram of adsorbent was mixed into the synthetic dye solution with a concentration of 25 ppm and a contact time of 180 minutes. Table 4 presents the results of the analysis.

Table 4. Analysis Results of pH and Color Before and After the Adsorption Process

Sample	**pH**	**Color (Pt.co)**
Before Adsorption	8.41	1843
After Adsorption	9.17	157

Table 4 shows that the initial pH was 8.41. After the adsorption process, the pH increased to 9.17, indicating a shift to a more alkaline environment, likely due to interactions between the contaminants and the adsorbent. The color, measured in Pt.co units, showed a significant decrease from 1843 Pt.co to 157 Pt.co. This drop highlights the high effectiveness of the adsorbent in removing particles or dye that caused turbidity. This suggests that palm shell activated carbon as an adsorbent can reduce turbidity and modify the pH of dye-laden wastewater. It demonstrates that adsorption is an economical and efficient method for industrial wastewater treatment, especially for addressing color pollution in wastewater (Velusamy et al., 2021).

The results of this study were compared with previous studies that utilized similar materials, such as rice husk and sawdust. For example, the study by Zhang et al. (2022) demonstrated that rice husk-based adsorbents achieved an adsorption capacity of up to 80% for similar dye compounds but required a longer contact time compared to the palm shell adsorbents tested in this study. Additionally, the study by Wu et al.

(2024) on sawdust showed an adsorption efficiency of up to 82% under different drying conditions. This comparison highlights that the modified palm shell material has the advantage of a shorter contact time while maintaining high adsorption efficiency.

CONCLUSION

Drying palm shells at an optimal temperature of 80°C for 4 hours is effective in reducing moisture content without damaging the pore structure of the material, enhancing the adsorption capacity of palm shells for industrial applications. The exponential model accurately predicted the drying rate.

FTIR results revealed the presence of -OH, C=O, and M-O functional groups on the activated carbon surface, supporting increased adsorption capacity for organic compounds. XRD analysis indicated a higher amorphous component, contributing to enhanced surface area and adsorption capacity. This combination of modifications makes palm shell-based activated carbon a promising adsorbent material for industrial wastewater treatment.

This study has several limitations, particularly regarding the variation in drying temperature and the non-uniformity of palm kernel shell particle sizes, which may affect the overall adsorption results. Therefore, further research can be conducted with different drying temperature variations or by developing more uniform adsorbent particle sizes to enhance adsorption efficiency. Additionally, further characterization, such as BET analysis and SEM, is needed on the dried palm kernel shell to better understand the changes in pore structure and their relationship with adsorption capacity.

ACKNOWLEDGEMENTS

We would like to thank the Ministry of Education, Culture, Research, and Technology of the Republic of Indonesia for the funding provided through the Beginner Lecturer Research scheme for the 2024 fiscal year (Contract No: 104/E5/PG.02.00.PL/2024 and 010/UTS/LP/B.06/Plg/2024).

REFERENCES

Aksoy, A., Karasu, S., Akcicek, A., & Kayacan, S. (2019). Effects of different drying methods on drying kinetics, microstructure, color, and the rehydration ratio of minced meat. *Foods*, *8*(6). https://doi.org/10.3390/foods8060216

Alsulami, R. A., El-Sayed, S. A., Eltaher, M. A., Mohammad, A., Almitani, K. H., & Mostafa, M. E. (2023). Thermal decomposition characterization and kinetic parameters estimation for date palm wastes and their blends using TGA. *Fuel*, *334*. https://doi.org/10.1016/j.fuel.2022.126600

Andrade, C., Delgado, J. M. P. Q., & Mesquita, E. F. T. (2022). Modeling and simulation of drying kinetics/curves: application to building materials. *Journal of Building Pathology and Rehabilitation*, *7*(8).

Boateng, I. D., & Yang, X. M. (2021). Process optimization of intermediate-wave infrared drying: Screening by Plackett–Burman; comparison of Box-Behnken and central composite design and evaluation: A case study. *Industrial Crops and Products*, *162*. https://doi.org/10.1016/j.indcrop.2021.113287

Broda, M., Curling, S. F., & Frankowski, M. (2021). The effect of the drying method on the cell wall structure and sorption properties of waterlogged archaeological wood. *Wood Science and Technology*, *55*(4), 971–989.

https://doi.org/10.1007/s00226-021-01294-6

Bulavchenko, O. A., & Vinokurov, Z. S. (2023). In Situ X-ray Diffraction as a Basic Tool to Study Oxide and Metal Oxide Catalysts. In *Catalysts* (Vol. 13, Issue 11). Multidisciplinary Digital Publishing Institute (MDPI). https://doi.org/10.3390/catal13111421

Dolah, R., Karnik, R., & Hamdan, H. (2021). A comprehensive review on biofuels from oil palm empty bunch (Efb): Current status, potential, barriers and the way forward. In *Sustainability (Switzerland)* (Vol. 13, Issue 18). MDPI. https://doi.org/10.3390/su131810210

Gayathiri, M., Pulingam, T., Lee, K. T., & Sudesh, K. (2022). *Activated carbon from biomass waste precursors: Factors affecting 1 production and adsorption mechanism*.

Macedo, L. L., Vimercati, W. C., Araújo, C. da S., Saraiva, S. H., & Teixeira, L. J. Q. (2024). Effect of drying air temperature on drying kinetics and physicochemical characteristics of dried banana. *Food Process Engineering*, *47*(9).

Mehdipour-Ataei, S., & Aram, E. (2023). Mesoporous Carbon-Based Materials: A Review of Synthesis, Modification, and Applications. In *Catalysts* (Vol. 13, Issue 1). MDPI. https://doi.org/10.3390/catal13010002

Mortada, W. I., Mohamed, R. A., Monem, A. A. A., Awad, M. M., & Hassan, A. F. (2023). Effective and Low-Cost Adsorption Procedure for Removing Chemical Oxygen Demand from Wastewater Using Chemically Activated Carbon Derived from Rice Husk. *Separations*, *10*(1). https://doi.org/10.3390/separations10010043

Radojčin, M., Pavkov, I., Kovačević, D. B., Putnik, P., Wiktor, A., Stamenković, Z., Kešelj, K., & Gere, A. (2021). Effect of selected drying methods and emerging drying intensification technologies on the quality of dried fruit: A review. In *Processes* (Vol. 9, Issue 1, pp. 1–21). MDPI AG. https://doi.org/10.3390/pr9010132

Setiajiati, F., Nurrochmat, D. R., Van Assen, B. W., & Purwawangsa, H. (2024). Current status of Indonesia's palm oil products and their competitiveness in the global market. *IOP Conference Series: Earth and Environmental Science*, *1379*(1). https://doi.org/10.1088/1755-1315/1379/1/012022

Thao, B. T. T., Vo, T. T. K., Tran, T. Y. N., Le, D. T., Tran, T. T., Bach, L. G., & Dao, T. P. (2023). Application of mathematical techniques to study the moisture loss kinetics and polyphenol degradation kinetics of mango (Mangifera indica L.) slices during heat pump drying by pilot equipment. *LWT*, *176*. https://doi.org/10.1016/j.lwt.2023.114454

Uchegbulam, I., Momoh, E. O., & Agan, S. A. (2022). Potentials of palm kernel shell derivatives: a critical review on waste recovery for environmental sustainability. In *Cleaner Materials* (Vol. 6). Elsevier Ltd. https://doi.org/10.1016/j.clema.2022.100154

Velusamy, S., Roy, A., Sundaram, S., & Kumar Mallick, T. (2021). A Review on Heavy Metal Ions and Containing Dyes Removal Through Graphene Oxide-Based Adsorption Strategies for Textile Wastewater Treatment. In *Chemical Record* (Vol. 21, Issue 7, pp. 1570–1610). John Wiley and Sons Inc. https://doi.org/10.1002/tcr.202000153

Wang, B., Lan, J., Bo, C., Gong, B., & Ou, J. (2023). Adsorption of heavy metal onto biomass-derived activated

carbon: review. In *RSC Advances* (Vol. 13, Issue 7, pp. 4275–4302). Royal Society of Chemistry. https://doi.org/10.1039/d2ra07911a

Wu, Z., Zhu, G., Peng, M., Zhu, Y., Miao, W., Li, D., Qin, D., Ma, P., & Chen, F. (2024). Kinetic analysis and calculation correction methods for moisture evaporation rate in pine lignocellulosic biomass. *Case Studies in Thermal Engineering*, *61*. https://doi.org/10.1016/j.csite.2024.104985

Xu, K., Li, Y., Xiong, J., Ou, X., Su, W., Zhong, G., & Yang, C. (2018). Activated Amorphous Carbon With High-Porosity Derived From Camellia Pollen Grains as Anode Materials for Lithium/Sodium Ion Batteries. *Frontiers in Chemistry*, *6*. https://doi.org/10.3389/fchem.2018.00366

Yek, P. N. Y., Liew, R. K., Osman, M. S., Lee, C. L., Chuah, J. H., Park, Y. K., & Lam, S. S. (2019). Microwave steam activation, an innovative pyrolysis approach to convert waste palm shell into highly microporous activated carbon. *Journal of Environmental Management*, *236*, 245–253. https://doi.org/10.1016/j.jenvman.2019.01.010

Yim, Y. J., & Kim, B. J. (2023). Preparation and Characterization of Activated Carbon/Polymer Composites: A Review. In *Polymers* (Vol. 15, Issue 16). Multidisciplinary Digital Publishing Institute (MDPI). https://doi.org/10.3390/polym15163472

Zhang, Q., Ye, Q., Zhang, Y., Cai, Q., Dang, Y., Pang, H., & Wu, X. (2022). High efficiency solar interfacial evaporator for seawater desalination based on high porosity loofah sponge biochar. *Solar Energy*, *238*, 305–314. https://doi.org/10.1016/j.solener.2022.04.044